



Internal multi-scale multi-physics coupled system for high fidelity simulation of light water reactors



A. Ivanov^{a,*}, V. Sanchez^a, R. Stieglitz^a, K. Ivanov^b

^aKarlsruhe Institute of Technology, Institute of Neutron Physics and Reactor Technology, Herman-vom-Helmholtz-Platz-1, 76344 Eggenstein-Leopoldshafen, Germany

^bThe Pennsylvania State University, Department of Mechanical and Nuclear Engineering, 206 Reber, University Park, PA 16802, USA

ARTICLE INFO

Article history:

Received 28 June 2013

Received in revised form 2 December 2013

Accepted 8 December 2013

Keywords:

Coupled codes

Stochastic approximation

Internal coupling

MCNP5

SUBCHANFLOW

Collision density estimator

ABSTRACT

In order to increase the accuracy and the degree of spatial and energy resolution of core design studies, coupled 3D neutronic (multi-group deterministic and continuous energy Monte-Carlo) and 3D thermal-hydraulic (CFD and subchannel) codes are being developed worldwide. At KIT, both deterministic and Monte-Carlo codes were coupled with subchannel codes and applied to predict the safety-related design parameters such as minimal critical power ratio (MCPR), maximal cladding and fuel temperature, departure from nuclide boiling ratio (DNBR). These coupling approaches were revised and considerably improved. Innovative method of internal on-the-fly thermal feedback interchange between the codes was implemented. It no longer relies on explicit material definitions and allows the modeling of temperature and density distributions based on the cell coordinates. In contrast to all existing coupled schemes, this method uses only standard MCNP geometry input and requires only proper definition of the geometrical dimensions. The initial material definition is arbitrary and is determined on-the-fly during the neutron transport by the thermal-hydraulic feedback. Another key issue addressed is the optimal application of parallel computing and the implementation of less time consuming tally estimators. Using multi-processor computer architectures and implementing collision density flux estimator, it is possible to reduce the Monte-Carlo running time and obtain converged results within reasonable time limit. The coupled calculation was accelerated further, by implementing stochastic approximation-based relaxation technique. Further, it is shown that large fuel assemblies can be analyzed on subchannel level.

© 2013 Elsevier Ltd. All rights reserved.

1. Introduction

High fidelity coupled solutions of neutron physics and thermal-hydraulic codes are being developed worldwide to increase the accuracy and the degree of spatial resolution of core design studies. For example coupled, Three-Dimensional (3D) neutronic (multi-group deterministic and continuous energy Monte-Carlo) and 3D thermal-hydraulic (CFD and subchannel) codes have been realized (Tippayakul et al., 2007; Watta et al., 2006; Puente-Espel et al., 2009, 2010). At the Karlsruhe Institute of Technology (KIT), both deterministic and Monte-Carlo codes have been coupled with subchannel codes and applied to predict the safety-related design parameters such as pin power, maximum cladding and fuel temperature of a PWR fuel assembly at nominal conditions (Sánchez et al., 2008; Sanchez and Al-Hamry, 2009).

The research done on the topic however, is mainly limited to small problems consisting of only few pins and based on external

coupling of the involved codes. For such problems the stability of the coupled system is not effectively tested. In the case of large problems consisting of many thousands of cells, achieving convergence of the coupled calculation, convergence of the fission source and proper statistics poses a real challenge. The existing coupled schemes are affected by the inability of some Monte-Carlo codes, such as MCNP, to model three dimensional (3D) distributions of density and temperature. In practical terms, the definition of large numbers of cells with distinct material specifications is required, a serious drawback resulting in large input files. This approach seriously limits the flexible geometry definition of Monte-Carlo codes. The main application of such a coupled system is to provide reference solutions, to serve as numerical benchmark and to validate deterministic calculations of complex fuel assembly designs, where the homogenization theory requires reliable validation. Therefore, having this in mind one requires the ability to model large problems within a consistent coupled system.

In the current paper, the further development and improvement of the KIT coupling approaches will be presented. In addition the effects of the stochastic approximation method on the convergence of the coupled scheme will be presented. Using this new

* Corresponding author.

E-mail addresses: aleksandar.ivanov@kit.edu (A. Ivanov), vector.sanchez@kit.edu (V. Sanchez), robert.stieglitz@kit.edu (R. Stieglitz), kni1@psu.edu (K. Ivanov).

acceleration method, it is possible to achieve uniform convergence. In addition, it is shown how the degree of convergence depends only on the number of coupled iterations.

The innovative internal coupling scheme implemented recently in MCNP5/SUBCHANFLOW, enabling the cell-wise definition of density and temperature distributions, will be presented. Using this innovative coupling approach it is no longer necessary to define massive MCNP inputs, when distribution of densities and temperatures are required. The MCNP input is kept as simple as possible and it can be built by using only standard MCNP features. In the framework of the new internal coupling scheme the neutrons obtain their feedback information on the fly as they explore the geometry. This strategy is applied to both single differential and double differential data.

2. Codes used in the coupled calculations

The Monte-Carlo code MCNP5 and the thermal-hydraulic subchannel code SUBCHANFLOW are selected for these investigations. In addition, NJOY modules LEAPR, THERMR, ACER and BROADR are used to process the nuclear data.

2.1. The thermal-hydraulic subchannel code SUBCHANFLOW

For performing the subchannel analysis, SUBCHANFLOW (SCF), a code under development at the KIT, was employed (Sanchez et al., 2010; Imke and Sanchez, 2012). It is based on the COBRA code family and is able to treat hexagonal and square bundle geometries with axially varying cell size. SUBCHANFLOW is written in FORTRAN 95 language in a fully modular way. Global data structure as well as fluid and material properties are stored in separate modules. The code solves mass, axial momentum, lateral momentum and energy conservation equations for vertical flow conditions. SUBCHANFLOW supports water, lead, helium, lead-bismuth and sodium as working fluid. Using thermal-hydraulic modeling based on 3 equations approach. Recently, a boron transport model and a point kinetics model have been implemented.

2.2. The neutronic code MCNP5 and the nuclear data processing code NJOY

MCNP5 simulates neutron transport in three dimensions using the Monte-Carlo method (Brown, 2005; MCNP, 2004). In the coupled run MCNP5 is used to generate the power profile, which is then transferred to SUBCHANFLOW. In order to read the power profile the newly implemented collision density estimator for the cell tally (Fx:n) and mesh tally (FMESH4:n) are used. In addition, the nuclear data processing code NJOY99 was used. The module BROADR (NEA/NSC/DOC, 2006) was used for Doppler-broadening of the continuous energy cross sections. In addition to the BROADR module, the LEAPR-THERMR-ACER module sequence was used for preparing thermal scattering data at different temperatures.

3. Coupled Monte-Carlo – thermal-hydraulic calculations

3.1. Mathematical definition of the problem

The steady-state neutron transport equation with no external sources can be transformed into integral form (1), the complete derivation can be found in Spanier and Gelbart, (1969), Lewis and Miller, (1984).

$$\varphi(\zeta) = \iint_{\Gamma} K(\zeta, \zeta') \varphi(\zeta') d\zeta' \quad (1)$$

Here Γ denotes the integration domain of the phase space and ζ represents the phase space variables. This is a Fredholm integral

equation. Being a fixed point problem the existence of solution is determined by the Banach fixed point theorem (Dunford and Schwartz, 1958), (Kolmogorov and Fomin, 1963):

Theorem 1. Let \mathcal{M} be a complete metric space with distance between two points A and B given by $\rho(A, B)$. Moreover, let $\mathcal{L} : \mathcal{M} \rightarrow \mathcal{M}$ be a contraction operator, for which there exists $k \in (0, 1)$ such that for all $A, B \in \mathcal{M}$, $\rho(\mathcal{L}(A), \mathcal{L}(B)) \leq k\rho(A, B)$. Then, there exists a unique $A \in \mathcal{M}$ such that $\mathcal{L}(A) = A$. The point A , can be generated by the iteration $\mathcal{L}(A_{n-1}) = A_n$, with A_0 being arbitrary.

Here the distance is defined to have the following properties: For all $A, B, C \in \mathcal{M}$, $\rho(A, A) = 0$, $\rho(A, B) \geq 0$, $\rho(A, B) = \rho(B, A)$ and $\rho(A, B) \leq \rho(A, C) + \rho(B, C)$.

These important properties of the space \mathcal{M} allow us to define convergence. In fact, the proof of the theorem is based on showing that $\rho(A_n, A_m)$ for $A_n, A_m \in \mathcal{M}$ is a Cauchy sequence converging due to the metric space \mathcal{M} being complete by definition. Therefore, the following limit exists (2)

$$\begin{aligned} \lim_{n \rightarrow \infty} A_n &= \lim_{n \rightarrow \infty} \mathcal{L}(A_{n-1}) \\ A_* &= \mathcal{L}(A_*) \end{aligned} \quad (2)$$

The Banach fixed point theorem gives important insight into the solutions of (1) and the space they reside on. It should be noted that to fulfill the conditions of a contraction operator, the kernel of the integral transport equation should be bounded and continuous (Dunford and Schwartz, 1958).

As pointed out in Dufek and Gudowski, (2006), the estimation of the power profile distribution results in the solution of the following problem (3)

$$\varphi = G(T(\varphi), H(\varphi)), \quad (3)$$

where $H(\varphi)$ and $T(\varphi)$ are the density and temperature distributions and the value of $G(T(\varphi), H(\varphi))$ is estimated by the Monte Carlo codes with superimposed statistic noise ε . The Monte-Carlo estimate of the left hand side of (3) is defined as (4)

$$Y(\varphi) = G(T(\varphi), H(\varphi)) + \varepsilon \quad (4)$$

The problem as given by (3) can be in principle solved by an iterative scheme, consecutively updating $H(\varphi)$ and $T(\varphi)$. However, this is a very inefficient method. Moreover, the convergence will be limited by the magnitude of ε . Therefore, in order to achieve convergence one must run large number of iterations applying huge number of particle histories. Based on this, it is recommended to use an acceleration scheme. In the past relaxation scheme, acting on the thermal-hydraulic parameters only, has been used (Watta et al., 2006; Hooogenboom et al., 2011). The old relaxation scheme is described by the equation set (5), where “ i ” is the iteration step number.

$$\begin{aligned} T_{\text{fuel}, i+1}^{\text{weighted}} &= (1 - \omega) T_{\text{fuel}, i-1} + \omega \left(T_{\text{fuel}, i}^{\text{actual}} \right), \\ T_{\text{H}_2\text{O}, i+1}^{\text{weighted}} &= (1 - \omega) T_{\text{H}_2\text{O}, i-1}^{\text{actual}} + \omega \left(T_{\text{H}_2\text{O}, i}^{\text{actual}} \right), \\ \rho_{\text{H}_2\text{O}, i+1}^{\text{weighted}} &= (1 - \omega) \rho_{\text{H}_2\text{O}, i-1}^{\text{actual}} + \omega \left(\rho_{\text{H}_2\text{O}, i}^{\text{actual}} \right). \end{aligned} \quad (5)$$

This scheme accelerates the solution. Unfortunately the convergence rate is still correlated to the statistical noise. The natural method of acceleration for problem (3) is to use a stochastic approximation technique. Although the same method of acceleration as in Dufek and Gudowski, (2006) is used, different reasoning concerning its applicability is applied. The theorem of Robbins and Monro is to be stated hereafter. The formulation of the theorem as well as the proof can be found in Wasan, (1969). The basic idea is, that by observing random variables $Y(X_n)$ of an unknown distribution, roots of the unknown underlying distribution can be found. In the particular case this is the estimate of (4).

Theorem 2. Let \mathcal{K} be a distribution function and α a real number such that there is a real number X giving $\mathcal{K}(X) = \alpha$; let \mathcal{K} be differentiable at X and $\mathcal{K}'(X) > 0$. Let X_1 be a real number and n be a positive integer. Let

$$X_{n+1} = X_n - \frac{1}{n}(\alpha - Y(X_n)), \quad (6)$$

where $Y(X_n)$ is a random variable such that the following conditional probabilities hold

$$\begin{aligned} P[Y_n = 1 | X_1, X_2, \dots, X_n, Y_1, Y_2, \dots, Y_{n-1}] &= \mathcal{K}(X_n), \\ P[Y_n = 0 | X_1, X_2, \dots, X_n, Y_1, Y_2, \dots, Y_{n-1}] &= 1 - \mathcal{K}(X_n). \end{aligned} \quad (7)$$

Then $\lim_{n \rightarrow \infty} E(X_n - X)^2$, so that the random sequence X_n converges in probability to X .

Since a fixed source problem is being discussed $\mathcal{K}(X) = \alpha$ transforms to $\mathcal{K}(X) = X$ and (6) to

$$X_{n+1} = X_n - \frac{1}{n}(X_n - Y_n), \quad (8)$$

First of all, note that this theorem, as given is for functions operating on the real numbers. In this case, however, the solutions of (1) residing on some complete metric space, as defined by Theorem 1 are of interest. Therefore, it should be investigated whether the conditions of Theorem 2 are fulfilled on the complete metric space \mathcal{M} . Since in essence the theorem of Robbins-Monro is proven by showing that the sequence $\xi_n = E(X_n - X)^2$ has limit $\lim_{n \rightarrow \infty} \xi_n = 0$ the possibility to define metric that allows convergence on \mathcal{M} is required. This is obviously possible due to the conditions of the Banach theorem. It remains to be show $\mathcal{K}'(X) > 0$. This is very challenging, because the exact form of $\mathcal{K}(X)$ or in the concrete case $G(T(\varphi), H(\varphi))$ is not known. However, Eqs. (1) and (3) are estimates of the same object φ . Based on that, $G(T(\varphi), H(\varphi))$ from the right-hand-side (RHS) of (3) can be identified with the left-hand-side (LHS) of (1). Applying the Gateaux derivative to the RHS of (1) and using the linearity of integration one obtains

$$\begin{aligned} D_{\phi(\xi')} F(\phi(\xi)) &= \lim_{\epsilon \rightarrow 0} \frac{F(\phi(\xi) + \epsilon \delta(\xi - \xi')) - F(\phi(\xi))}{\epsilon} \\ &= \int K(\xi', \xi) \delta(\xi' - \xi) d\xi' > 0. \end{aligned} \quad (9)$$

The last result (8) tells us, that the positivity of the derivative is ensured by the positivity of the kernel. In addition the solutions of (1) are assumed to be continuous functions, based on physical arguments. In (9) the notation was simplified by denoting the RHS of (1) by the linear operator $F(\varphi)$.

Based on the above considerations, the Robbins-Monro theorem can be applied to the original problem. Here Y_n from (8) is the Monte Carlo estimate of $G(T(\varphi), H(\varphi)) + \epsilon$, i.e. Eq. (4).

There exists an additional argument confirming the applicability of the Robbins-Monro theorem. Consider the following equivalent formulation Theorem 2.1 (Bauer, 1990), of Theorem 2. Let the sequence (10) being iterative estimate of the equation $K(\theta) = \alpha$

$$X_{n+1} = X_n - \gamma_n(\alpha - Y(X_n)), \quad (10)$$

where the following conditions on γ_n are imposed (11)

$$\sum_{n=1}^{\infty} \gamma_n = \infty, \quad \sum_{n=1}^{\infty} \gamma_n^2 < \infty. \quad (11)$$

Choosing $\gamma_n = 1/n$ and using the Cauchy integral convergence test, one can easily show that the conditions (11) are fulfilled for this choice of γ_n .

Theorem 2.1. If $\mathcal{K}(X)$ and $Y(X)$ fulfill the following conditions

$$\forall X \in \mathfrak{R} : |\mathcal{K}(X)| \leq A|X| + B, \quad (A, B \in \mathfrak{R}), \quad (12)$$

$$E[Y(X) - \mathcal{K}(X)] < \infty, \quad (13)$$

$$\forall \epsilon \in (0, 1), \forall X : 1/\epsilon > |X - \theta| > \epsilon \Rightarrow \inf_X |\mathcal{K}(X) - \theta| > 0. \quad (14)$$

The limit $\lim_{n \rightarrow \infty} E(X_n - \theta)^2 = 0$ exists.

The theorem has to be proven applicable to the particular case (3). Since a fixed point problem is being discussed, $\mathcal{K}(\theta) = \alpha$ translates to $\mathcal{K}(\theta) = \theta$. As already shown, Theorem 1 allows the definition of metric on the solution space of (3) and the limit $\lim_{n \rightarrow \infty} E(X_n - \theta)^2$ can be studied. Theorem 2.1, however, requires proving the additional conditions (12)–(14). Condition (12) holds since $G(T(\varphi), H(\varphi))$ has to be a contraction operator. According to Theorem 1, choosing any φ, φ' , one obtains (15)

$$|G(T(\varphi), H(\varphi)) - G(T(\varphi'), H(\varphi'))| \leq A|\varphi - \varphi'|. \quad (15)$$

Since φ and φ' are arbitrary let $\varphi' = 0$. If $\varphi' = 0$ one obtains $G(T(\varphi'), H(\varphi')) = 0$. Then (16) follows, the real constant is in this case $B = 0$

$$|G(T(\varphi), H(\varphi))| \leq A|\varphi|. \quad (16)$$

The condition (13) holds since the counterparts of $K(X)$ and $Y(X)$, $G(T(\varphi), H(\varphi))$ and $Y(\varphi)$ are both bounded and they differ only by the stochastic noise. The interval $\frac{1}{\epsilon} > |X - \theta| > \epsilon$ translates to compact in the space of φ Moreover $G(T(\varphi), H(\varphi))$ is continuous and $G(T(\varphi), H(\varphi)) \neq \varphi$ for all $\varphi = \varphi^*$, where φ^* is the fixed point of interest. Therefore the minimum of $|G(T(\varphi), H(\varphi)) - \varphi|$ is attained on a compact and $\inf_X |G(T(\varphi), H(\varphi)) - \varphi| > 0$, (14) follows.

As pointed out in (Dufek and Gudowski, 2006) Eq. (8) can be further simplified. The notation in (8) is adapted for the case of the flux

$$\varphi^{(n+1)} = \left(1 - \frac{1}{n}\right) \varphi^{(n)} + \frac{1}{n} Y(\varphi_n). \quad (17)$$

Eq. (17) simplifies to (18)

$$\varphi^{(n+1)} = \frac{1}{n} \sum_{i=1}^n Y(\varphi_i). \quad (18)$$

This can be easily shown by induction, first assume (18) holds for n and then check if it holds for $n + 1$. Substituting (18) in (17) the following equation is obtained. (19)

$$\varphi^{(n+1)} = \left(1 - \frac{1}{n}\right) \frac{1}{n-1} \sum_{i=1}^{n-1} Y(\varphi_i) + \frac{1}{n} Y(\varphi_n) = \frac{1}{n} \sum_{i=1}^n Y(\varphi_i). \quad (19)$$

Formula (18) is the main result of this paper. It gives us the explicit formulation of the relaxation scheme. The flux (power profile) in the next iteration is obtained to be the mean value of all iterations. Since in essence the tally estimates from all the runs are added together, simple error propagation with partial derivatives on (18) shows the error decreases with increasing the number of iterations. Moreover, from (18) follows that all iterations are reflected in the final solution with weight of $1/n$. Therefore, any desired convergence parameter can be achieved, if enough number of iterations is run. This is still possible even at low number of histories. Nevertheless the number of histories and the number of inactive cycles should be chosen adequate to ensure the fission source convergence. Moreover, the effect of increasing the number of histories in the old scheme is achieved by running larger number of iterations in the new scheme.

4. Description of the internal coupled scheme

4.1. Internal coupling via memory

Coupled Monte-Carlo neutronic calculations are to be described in this paper. In such calculations one repeatedly updates the power profile distribution estimated by the neutronics code, in

accordance with the changing thermal–hydraulics distribution estimated by the deterministic code. These iterations are repeated until the desired degree of convergence is met. Details of the calculation flow are given in Ivanov et al., (2013). Calculation flow of the coupled system is shown in Fig. 1.

In MCNP there exists no option to define temperature and density distribution. Therefore, all existing coupled schemes rely on explicit geometry definition. Using this method one ends up defining explicitly all cells, where the thermal–hydraulic boundary conditions are to be updated. Although straightforward, this method is not very practical and it results in massive input files. As an illustrative example one can consider the study case of this paper. It consists of 16,380 cells with thermal–hydraulic feedback. To define them explicitly one needs 16,380 lines, only for the geometry definition. However, the geometry distribution is only one part of the problem. To define the temperature distribution, one needs a distinct material composition in each cell. This will increase the total number of input lines to over 200,000. Clearly, another strategy for the coupling is needed. In this paper an additional option in MCNP, allowing the definition of temperature and density distributions is to be presented. All serious MCNP calculations should be run in parallel. Therefore, our scheme is written and will be described in the framework of parallel computing.

As initial step SCF was included as a subroutine in the MCNP code, allowing the interchange of feedback parameters via a FORTRAN module. SCF is run on the master node, and once it finishes a specially defined subroutine selects the necessary Doppler broadened nuclear cross sections. In order to enable the selection, all necessary nuclear data must be preloaded into the memory by the master process. In the case of incoherent inelastic scattering on bound nuclei, the additional thermal scattering data has to be supplied in addition. It should be noted, that the selection is done

only once and ready to use arrays are supplied for the subsequent transport calculation. This prohibits any computational time increase due to the cross-section selection process. All feedback relevant arrays are broadcasted by the master process to the slaves.

In the framework of the internal coupling it is no longer necessary to define explicit material distributions. At the beginning usual MCNP repeated structure input is defined. Actually, only one pin cell is defined and embedded in a 3D lattice to complete the geometry. At this moment only the proper geometric dimensions matter. The difference with respect to the standard MCNP input is the definition of a dummy material, used to load the necessary cross sections into the memory. The presence of this material is suppressed by modifying the source code. These cross sections are subsequently retrieved by the temperature interpolation subroutine.

Once the neutron transport starts, the neutrons see effective material distribution as defined by the thermal–hydraulics code. On-the-fly the neutron cross sections in each cell are overwritten, performing the stochastic mixing, without any reference to the actual input. This means that the starting materials present in the input, are substituted by pseudo mixtures evaluated at the proper cell temperature. This procedure is shown in Fig. 2. After this insertion the neutron transport process is conducted with macroscopic cross-sections evaluated at the proper cell temperature. The dynamic material distribution was enabled in the MCNP source by introducing custom designed subroutines for performing on-the-fly pseudo material mixing. This change of the cross sections as the neutron travels through the geometry, modifies the physical environment and introduces the feedback effects. The point of intervention is exactly before reactions are sampled and before the eigenvalue is computed, therefore, the initial materials present in the MCNP input are completely ignored. This modified step is shown on the right hand side of Fig. 3

The new method of coupling does not change the physics and must produce the same computational results as the usual MCNP code when the geometry is subdivided into cells, each having unique material, density and temperature. Testing the scheme is therefore quite simple. Two computations one defining the feedback via the standard method of explicit geometry definition and the other using the internal coupling scheme were run. Both methods produced completely identical results for both the multiplication factor and the power profile distribution. This has assured that the internal coupling scheme works correctly.

4.2. Temperature dependence of the nuclear data

Nuclear cross sections depend on relative velocity in the center of mass frame. Thermal oscillations of the target atomic nuclei, inducing changes of the relative velocity, result in the Doppler Effect, being one of the most important phenomena in nuclear reactor safety. From the thermal–hydraulic calculation, different material temperatures are supplied. Hence, the temperature effect on the corresponding nuclear cross sections should be considered. MCNP is capable of making corrections to the scattering cross section by supplying the kinetic energy corresponding to the most probable velocity of the target nucleus via the TMP card (van der Marck et al., 2005; Brown, 2005). This is however, not enough to treat the full temperature dependence.

A possible solution to the Doppler broadening of the nuclear data is to adapt online nuclear data processing, by running the NJOY module BROADR at each iteration step as proposed in Jouanne and Trama (2010), Tippayakul et al. (2007). However, in practical terms this approach results in large CPU times from running BROADR, and large memory demand to store the broadened data. In order to avoid this situation, another more practical approach was followed. In the actual MCNP calculation, the pseudo material

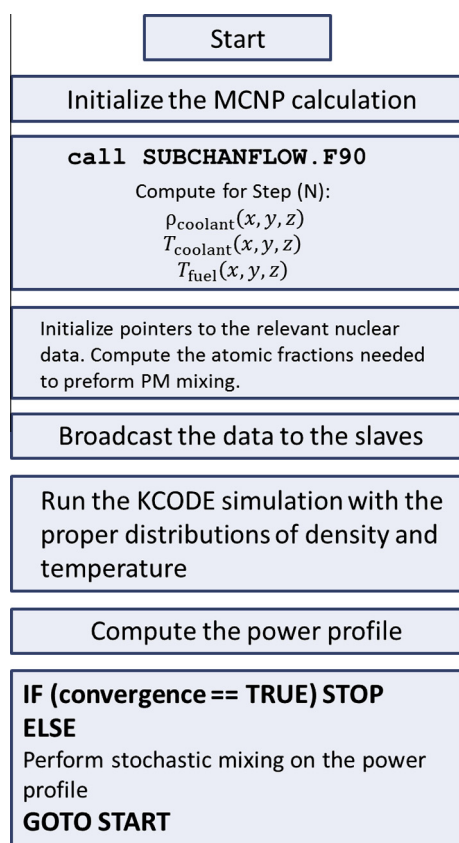


Fig. 1. Coupled calculation flow.

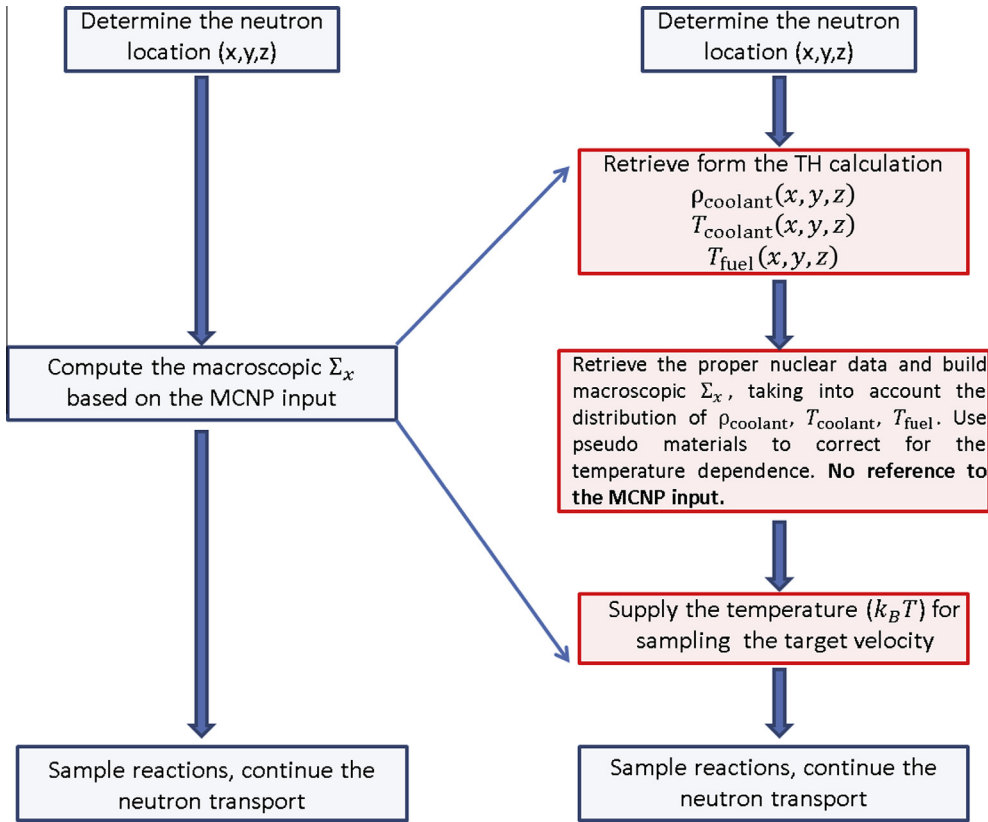


Fig. 2. On-the-fly thermal-hydraulic treatment in MCNP. The modified procedure is shown on the right hand side.

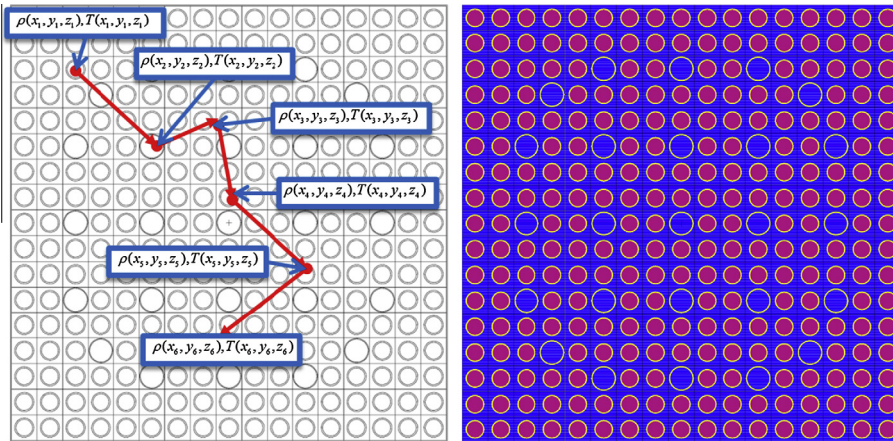


Fig. 3. Fuel temperature axial distribution for the last two coupled runs.

mixing was used to correct for the temperature dependence of the nuclear data during the coupled calculation. The two materials used in the mixture have temperatures, being the lower and the upper bound of the particular interval, in which the actual temperature obtained from SUBCHANFLOW is lying. For the atom fraction of the material obeying lower temperature the following weight is used (20)

$$f_{\text{low}} = \frac{\sqrt{T_{\text{high}}} - \sqrt{T_{\text{actual}}}}{\sqrt{T_{\text{high}}} - \sqrt{T_{\text{low}}}}. \quad (20)$$

For the higher temperature material (21) is used

$$f_{\text{high}} = 1 - f_{\text{low}}. \quad (21)$$

By using the pseudo material mixing approach one obtains the following cross section mixture (22)

$$\Sigma_{\text{pseudo}}(T_{\text{actual}}) = f_{\text{low}}\Sigma_{\text{low}}(T_{\text{low}}) + f_{\text{high}}\Sigma_{\text{high}}(T_{\text{high}}). \quad (22)$$

It should be taken into account that the pseudo material mixing is not interpolation in the classical sense. This method relies on the stochastic nature of the neutronics code and there exists no nuclear data generated at some intermediate temperature. When the individual neutrons enter specific cell, they can interact with a certain nuclide at a given temperature with probability defined by its atomic fraction.

In the framework of the internal coupling scheme all the necessary information how to perform the pseudo-material mixing (20)–(22) is assigned on the master node, and stored into arrays.

During the transport calculation this information is retrieved and applied to the specific cells based on the neutron coordinates.

In order to treat the thermal scattering from bound scatterers MCNP utilizes additional thermal scattering data files, prepared by the LEAPR-THERMR-ACER modules sequence of NJOY. While the Doppler broadening module BROADR is capable of producing cross-section files at all desired temperatures, LEAPR requires frequency spectrum of the scattering nucleus $\rho(\omega)$ for each temperature in order to generate the scattering law $S(\alpha, \beta)$. For the current study the LEAPR input given in (Mattes and Keinert, (2005) was used. In addition, the THERMR module of NJOY was used to generate the point-wise thermal scattering cross sections in PENDF format and the ACER module of NJOY was used to generate thermal scattering data for MCNP code in ACE format.

Since the temperatures at which the thermal scattering data can be prepared is predefined by the temperatures at which oscillation spectrum for the scattering nucleus exists, custom designed subroutine was used to refine the granularity of the $S(\alpha, \beta)$ temperature grid. This subroutine interpolates between thermal scattering files produced by the LEAPR-THERMR-ACER sequence. Thermal scattering files have been produced on a grid of 10 K increments. On the basis of these file the pseudo material mixing for the moderator was performed.

In the framework of the internal coupling, on the master node two types of information is assigned for the coolant. First, the information necessary to perform pseudo material mixing of the Doppler broadened data for the moderator isotopes is assigned. This method is based on (20)–(22). In addition to the usual single differential nuclear data references to the thermal scattering data libraries to be used for the different hydrogen evaluations are set. In each pseudo material mixture for the moderator two hydrogen evaluations are used, to each of them thermal scattering file is assigned. This information is retrieved during the subsequent transport run on the slaves. Graphical illustration of the pseudo material mixing for both single differentiable and double differentiable data is shown in Fig. 4. It should be taken into account that the thermal scattering data and the hydrogen evaluations, used for the pseudo material mixing in the moderator, are evaluated at the same temperature.

4.3. Tallying of the power profile distribution

MCNP uses the track-length estimator to tally the neutron fluxes. This method is very accurate and can be used to tally fluxes in all type of cells (including void cells). The definition is based on (Banerjee and Martin, 2012) the formula describing the track length estimator follows (23)

$$\psi = \frac{1}{NV} \sum_{i=1}^N \sum_{t=1}^{T_i} w_{i,t} d_{i,t}. \quad (23)$$

This estimator is having the meaning of the total distance traveled by the particles in the tally region multiplied by the weight of the particle and divided by the volume of the tally region. The second sum runs over the sequence of tracks for history “*i*” in the volume *V*. Here, $w_{i,t}$ and $d_{i,t}$ are the particle weight and distance

```

92238.xxc f_low      1001.iic f_low + therm.jjc
92235.xxc f_low      8016.iic f_low
 8016.xxc f_low      1001.jjc f_high + therm.jjc
92238.yyc f_high     8016.jjc f_high
92235.yyc f_high
 8016.yyc f_high

```

Fig. 4. Illustration of the pseudo material mixing for the single differentiable and the double differentiable nuclear data.

traveled, for history “*i*” and track “*t*”. Using track length estimator for flux tallying is very computationally expensive. Simple comparison between MCNP runs, with and without tallying reveals large computational time increase. For instance, running PWR with cell based tally assembly problem consisting of 5400 cells with 200,000 (200k) histories per cycle and 650 active cycles takes 4 h on 48 cores, if the track length tallying is done. Identical input without tallying takes about 30 min. The mesh tally, although much more efficient still increases the computational time significantly.

Since power tallying is done in high collision cells, without loss of precision, one can use the collision density estimator for flux tallying. The collision density estimator will give wrong results in the case when used in low density cells and is completely inapplicable for voided regions. The collision density estimator is defined by

$$\psi = \frac{1}{NV} \sum_{i=1}^N \sum_{c=1}^{C_i} \frac{w_{i,c}}{\Sigma_t(\zeta_{i,c})}. \quad (24)$$

Using this method, the flux is estimated by the total number of collisions for *N* histories in the volume *V* divided by the total cross-section. Here, the second sum runs over the sequence of collisions for history “*i*” in the volume *V*. $\zeta_{i,c}$ is the phase space vector for history “*i*” at collision event “*c*”.

The collision density estimator was implemented by modifying the tallying subroutine of MCNP. It was instructed to compute the ratio formulae (24) and accumulate the results every time, when the neutron undergoes a collision. Implementing the collision density estimator resulted in significant computational time decrease. Both the cell and the mesh tallies were modified to use the collision density estimator.

The reduced runtime is due to the less frequent calls of the tallying subroutine, namely, only when a collision has happened. It should be taken into account that the tallying procedure in MCNP is independent on the eigenvalue estimation. Therefore, no changes in terms of the eigenvalue were observed.

The implementation of the collision density estimator was validated by comparing it to the original track length estimator. The differences for all test cases were in the statistical uncertainty range. Tally estimates normalized to one source neutron as they are obtained by MCNP are shown in Fig. 5. The test case shown is a PWR pin problem.

Note that the difference shown on the LHS axis of Fig. 5 is computed using (25)

$$100 \times \left| \frac{P_{\text{track-length}} - P_{\text{collision-density}}}{P_{\text{track-length}}} \right|. \quad (25)$$

The performance of the tallies was tested on a quarter-core PWR model. Since it is quite well known that cell based tallies show very bad performance for large models, we have concentrated on testing the mesh tally. The mesh tally was set to accumulate scores in each pin cell. The geometry was subdivided into 20 axial zones. The following results, shown in Table 1 were obtained.

5. Verification of the coupled approach

5.1. Description of the verification model

As a test case a PWR fuel assembly was used. The thermal-hydraulic boundary conditions are given in Fig. 6. The new method of acceleration by stochastic approximation was tested against the old method of mixing the thermal-hydraulic parameters from two subsequent runs (5).

The old relaxation scheme was unstable and the convergence was strongly correlated to the tally relative errors. The following

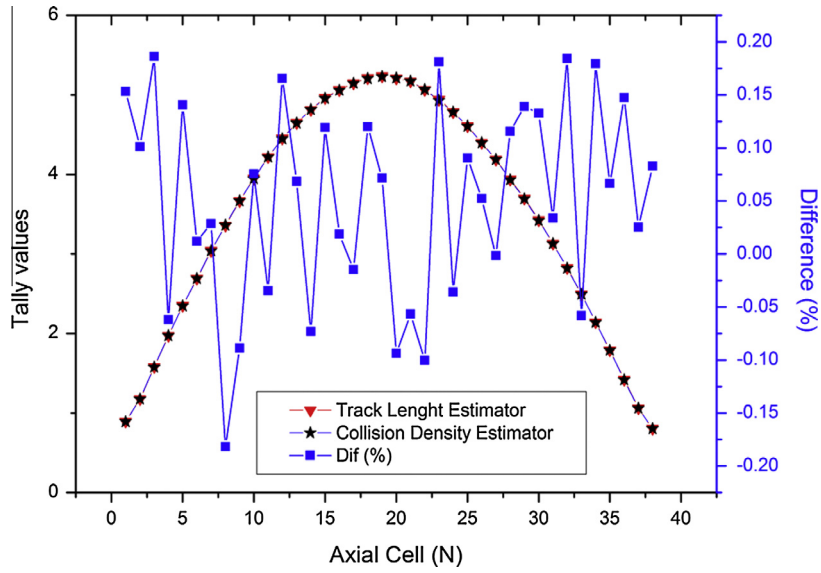
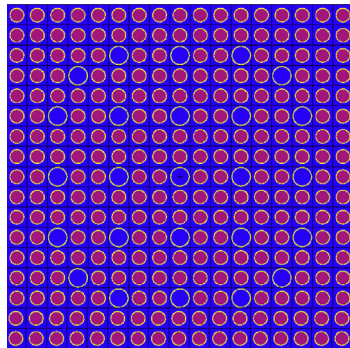


Fig. 5. Comparison of the track length estimator and the collision density estimator.

Table 1

Tally performance test.

No tallying	1 h:52 min	800k histories/cycle	600 criticality cycles
Track length FMESH	2 h:39 min	800k histories/cycle	600 criticality cycles
Collision density FMESH	2 h:10 min	800k histories/cycle	600 criticality cycles



Total length	3.71 m
Number of axial nodes	20
Inlet coolant temperature	563.15 K
Coolant mass flow rate	82.12 kg/s
Total power	18.47 MW
Exit pressure	15.375 MPa
Pin radius	0.4583 cm
Pellet radius	0.3951 cm
Guide tube radius	0.6032 cm
Boron Concentration	1500 ppm

Fig. 6. PWR assembly geometry layout cut and thermal-hydraulic boundary conditions.

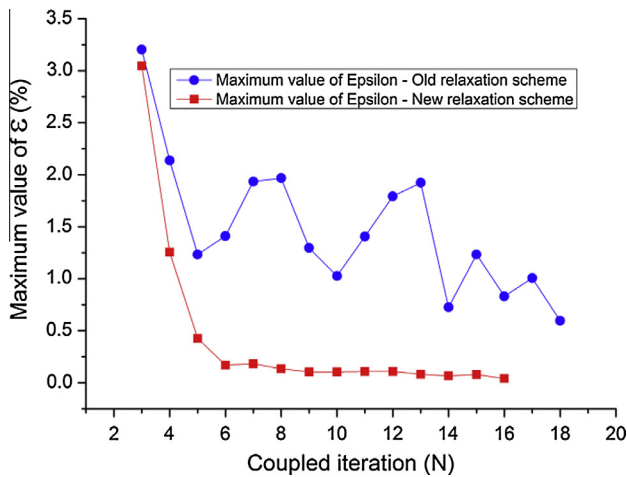


Fig. 7. Maximum value of the convergence parameter versus coupled iteration.

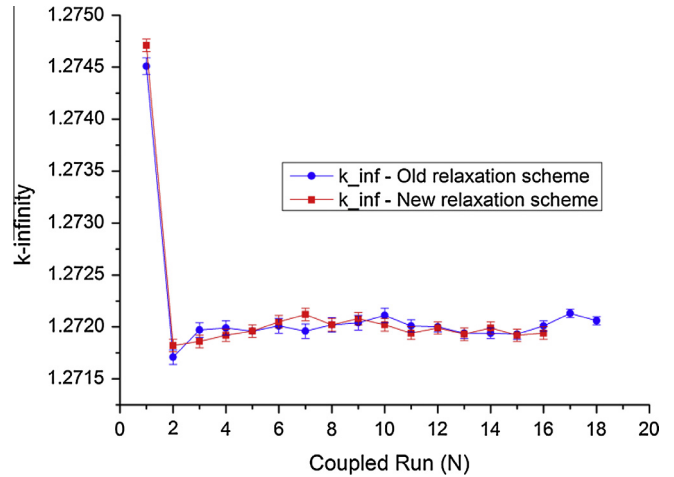


Fig. 8. k_{∞} versus coupled iteration number.

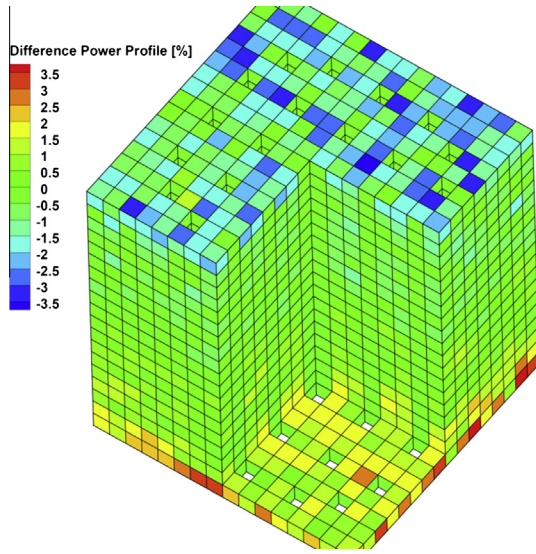


Fig. 9. Difference in the power profile produced by the two coupling schemes.

criterion (26) is imposed on the fuel temperature and is used as an estimate for convergence.

$$\varepsilon = 100 \times \left| \frac{T_{ij}^{\text{last}} - T_{ij}^{\text{prev}}}{T_{ij}^{\text{last}}} \right| \quad (26)$$

Here the index “i” is the pin number and “j” is the axial cell number. The indexes run over all pin cells in the problem. The thermal-hydraulic and neutronics iterations are repeated until the desired value for the convergence parameter is met. As evident from Fig. 7, the old relaxation scheme has limit of convergence given by the statistical uncertainty. It starts oscillating in the limit of ε

approaching the values for the tally relative errors. This oscillation will not disappear even when running very large number of iterations, unless the number of histories is increased. On the other hand, by using the stochastic approximation method the convergence parameter exhibits 1/N behavior. Using the new scheme, it was possible to achieve very fine convergence $\varepsilon = 0.04$. The old coupling scheme was stopped after 18 iterations and achieving $\varepsilon = 0.54$. Note the reduction of the oscillation amplitude, after running 14 coupled iterations. At this point the number of histories was doubled to ensure finer convergence. In contrast for the coupled iterations relying on stochastic approximation, where all iterations were run at constant number of histories. This is possible because all iterations are contained in the final results and the statistics is being improved after each coupled run.

The next important step is to check whether the new relaxation scheme induces any biasing of the results. By comparing the results for the multiplication factor close values for the two schemes were observed. For the converged runs, the piece-wise linear curve spanned by the k_∞ values should not leave the band defined by the multiplication factor’s standard deviation. Clearly this condition is violated for the old relaxation scheme (see Fig. 8).

Next the power profiles after achieving convergence, generated by the two schemes, were compared. As evident from Fig. 9 the differences are small and can be explained by the poor convergence of the old relaxation scheme. Moreover, the difference has maxima in the upper and lower parts of the fuel assembly, where the power profile estimates had large uncertainties. In the positions where the guide tubes are located, there is no power profile estimated, therefore the values are zero and were excluded from the plot.

Finally the results for the fuel temperature distribution and the coolant density are presented. The results are shown in Fig. 10. Note the position of the guide tubes on the LHS.

The calculations performed with the two relaxation schemes are summarized in Table 2. Note that the standard deviations of

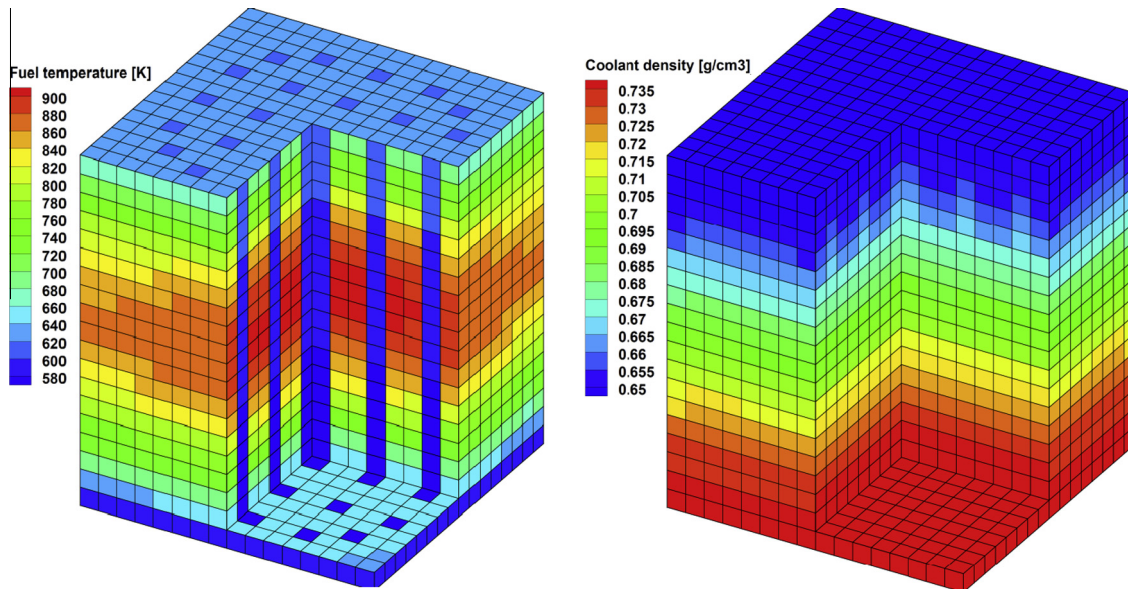


Fig. 10. Fuel temperature and coolant density distribution.

Table 2
Summary of the results.

Acceleration scheme	Histories	Active criticality cycles	Convergence	k_∞	Coupled iterations	Processors
Old	200k	600	$\varepsilon = 0.54$	1.27208(6)	18	48
New	200k	600	$\varepsilon = 0.04$	1.27194(5)	16	48

the eigenvalue estimates are given in brackets and have units of pcm.

6. Summary and outlook

In the current paper a novel internal coupling methodology between the Monte-Carlo code MCNP and the subchannel code SCF was presented. The newly developed scheme does not rely on the usual MCNP input description and enables the flexible definition of density and temperature distributions. In contrast to the external coupling schemes it does not require massive input files any more.

The convergence of the coupled scheme was accelerated and stabilized by applying stochastic acceleration strategy. Using the new method of acceleration it was possible to achieve $1/N$ convergence parameter evolution. Mathematical justification as well as numerical results were presented. For the test case, a 17×17 PWR fuel assembly consisting of 16,380 thermal-hydraulic feedback cells was chosen.

The collision density flux estimator was successfully implemented and was used to tally the power profile distribution. It was validated by comparing it to the standard track length estimator used in MCNP. The new tally option resulted in a speedup of the coupled simulations of three times compared to the simulation based on the track length estimator.

The peculiar features of the internal coupling approach for MCNP5/SUBCHANFLOW described above are necessary prerequisites for the simulation of whole cores at both fuel assembly and pin level in combination of massive parallel computing. In addition, this system is paving the way for depletion calculations taking into account the thermal-hydraulic feedbacks.

Acknowledgements

This research was partially funded by both the European Commission via the FP7 project HPMC “High-Performance Monte Carlo Reactor Core Analysis” under Contract no. 295971 and the Program Nuclear Safety Research of the Karlsruhe Institute of Technology and is embedded in the research work of the Institute of Neutron Physics and Reactor Technology (INR).

References

- Banerjee, K., Martin, W.R., 2012. Kernel density estimation method for Monte Carlo global flux tallies. *Nucl. Sci. Eng.* 170, 234–250.
- Bauer, H., 1990. *Wahrscheinlichkeitstheorie*, Walter deGruyter.
- Brown, F., 2005. *Fundamentals of Monte Carlo Particle Transport LA-UR-05-4983*. Los Alamos National Laboratory. <http://mcnp-green.lanl.gov/publication/pdf/LA-UR-05-4983_Monte_Carlo_Lectures.pdf>.
- Dufek, J., Gudowski, W., 2006. Stochastic approximation for Monte Carlo calculation of steady-state conditions in thermal reactors. *Nucl. Sci. Eng.* 152, 274–283.
- Dunford, N., Schwartz, J.T., 1963. *Linear Operators*. Interscience Publishers, New York (pt.I 1958, pt.II).
- Hoogenboom, E., Diop, Ch., Ivanov, A., Sanchez, V., 2011. Development of coupling methodologies for TRIPOLI and FLICA in the frame of NURISP Project. In: The 2011 International Conference on Mathematics and Computational Methods Applied to Nuclear Science and Engineering (M&C 2011), Rio de Janeiro, RJ, Brazil, May 8–12, 2011.
- Imke, U., Sanchez, V., 2012. Validation of the Subchannel Code SUBCHANFLOW Using the NUPEC PWR Tests (PSBT). *Science and Technology of Nuclear Installations*, vol. 2012, Article ID 465059, 12 pages. doi: 10.1155/2012/465059.
- Ivanov, A., Sanchez, V., Stieglitz, R., Ivanov, K., 2013. High fidelity simulation of conventional and innovative LWR with the coupled Monte-Carlo thermal-hydraulic system MCNP-SUBCHANFLOW. *Nucl. Eng. Des.* 262, 264–275.
- Jouanne, C., Trama, J., 2010. Linux Binary of TRIPOLI-4 capable of producing point cross-sections at various temperatures. NURISP Deliverable D.1.1.1., April 2010.
- Kolmogorov, A.N., Fomin, S.V., 1963. *Elements of the Theory of Functions and Functional Analysis*. Graylock Press.
- Lewis, E.E., Miller Jr., W.F., 1984. *Computational Methods of Neutron Transport*. John Wiley & Sons.
- Mattes, M., Keinert, J., 2005. Thermal Neutron Scattering Data for the Moderator Materials H₂O, D₂O and ZrHx in ENDF-6 Format and as ACE Library for MCNP(X) Codes. IAEA Nuclear Data Section, Wagramer Strasse 5, A 1400 VIENNA, April 2005, INDC(NDS)-0470.
- MCNP, 2004. *A General Monte Carlo N-Particle Transport Code, Version 5*. Los Alamos National Laboratory.
- Processing of the JEFF-3.1 Cross Section Library into Continuous Energy Monte Carlo Radiation Transport and Criticality Data. Library. NEA/NSC/DOC, 2006, p. 18.
- Puente-Espel, F., Avramova, M., Ivanov, K., Misu, St., 2009. High accuracy modeling for advance nuclear reactor core designs using Monte Carlo based coupled calculations, Invited paper for M&C 2009, Saratoga Springs, New York, May 3–7, 2009.
- Puente-Espel, F., Avramova, M., Ivanov, K., 2010. New developments of the MCNP/CTF/NEM/NJOY Code system-Monte Carlo based coupled code for high accuracy modeling. In: *Proceedings of Advances in Reactor Physics to Power the Nuclear Renaissance (PHYSOR)*, Pittsburgh, Pennsylvania, USA, May 9–14, 2010.
- Sanchez, V., Al-Hamry, A., 2009. Development of a coupling scheme between MCNP and COBRA-TF for the prediction of the pin power of a PWR fuel assembly. In: *Proceedings of International Conference on Mathematics, Computational Methods & Reactor Physics (M&C 2009)*, New York, USA.
- Sánchez, V., Al-Hamry, A., Broeders, C.H.M., 2008. Development and qualification of the coupled code system COBRA-TF/THREEDANT for the pin-by-pin power calculation. In: *Proceedings of ICAPP '08*. Anaheim, CA USA, June 8–12, 2008, Paper 8269.
- Sanchez, V., Imke, U., Gomez, R., 2010. SUBCHANFLOW: a thermal-hydraulic sub-channel program to analyse fuel rod bundles and reactor cores. In: *Proceedings of the 17th Pacific Basin Nuclear Conference*, Cancun, Mexico, October 2010, pp. 24–30.
- Spanier, J., Gelbard, E., 1969. *Monte Carlo Principles in Neutron Transport Problems*. Addison-Wesley.
- Tippayakul, C., Avramova, M., Puente Espel, F., Ivanov, K., 2007. Investigations on Monte Carlo based coupled core calculations. In: *Proceedings of ICAPP 2007*, Nice, France, May 13–18, 2007, Paper 7134.
- van der Marck, S., Meulekamp, R., Hogenbirk, A., 2005. New temperature interpolation in MCNP. In: *Proceedings of M&C 2005 conference*, Avignon, France.
- Wasan, M.T., 1969. *Stochastic Approximation*. Cambridge University Press.
- Watta, C., Schulenburg, T., Cheng, X., 2006. Coupling of MCNP With a Sub-Channel Code For Analysis of a HPLWR Fuel Assembly. FZKA7233, FZK, Karlsruhe Germany.